BJP British Journal of Pharmacology

DOI:10.1111/bph.12845
www.brjpharmacol.org

RESEARCH PAPER

Identification of novel insulin mimetic drugs by quantitative total internal reflection fluorescence (TIRF) microscopy

Peter Lanzerstorfer[1,*], Verena Stadlbauer[1,*], Lilia A Chtcheglova[2], Renate Haselgrübler[1], Daniela Borgmann[3], Jürgen Wruss[1], Peter Hinterdorfer[2,4], Klaus Schröder[5], Stephan M Winkler[3], Otmar Höglinger[1] and Julian Weghuber[1]

[1]*School of Engineering and Environmental Sciences, University of Applied Sciences Upper Austria, Wels, Austria,* [2]*Center for Advanced Bioanalysis GmbH, Linz, Austria,* [3]*School of Informatics, Communications and Media, University of Applied Sciences Upper Austria, Hagenberg, Austria,* [4]*Institute of Biophysics, Johannes Kepler University of Linz, Linz, Austria, and* [5]*BioMed zet Life Science GmbH, Linz, Austria*

Correspondence
Julian Weghuber, School of Engineering and Environmental Sciences, University of Applied Sciences Upper Austria, Stelzhamerstrasse 23, A-4600 Wels, Austria. E-mail: julian.weghuber@fh-wels.at

*Peter Lanzerstorfer and Verena Stadlbauer contributed equally to this work.

Received
4 February 2014
Revised
18 June 2014
Accepted
27 June 2014

BACKGROUND AND PURPOSE

Insulin stimulates the transport of glucose in target tissues by triggering the translocation of glucose transporter 4 (GLUT4) to the plasma membrane. Resistance to insulin, the major abnormality in type 2 diabetes, results in a decreased GLUT4 translocation efficiency. Thus, special attention is being paid to search for compounds that are able to enhance this translocation process in the absence of insulin.

EXPERIMENTAL APPROACH

Total internal reflection fluorescence (TIRF) microscopy was applied to quantify GLUT4 translocation in highly insulin-sensitive CHO-K1 cells expressing a GLUT4-myc-GFP fusion protein.

KEY RESULTS

Using our approach, we demonstrated GLUT4 translocation modulatory properties of selected substances and identified novel potential insulin mimetics. An increase in the TIRF signal was found to correlate with an elevated glucose uptake. Variations in the expression level of the human insulin receptor (hInsR) showed that the insulin mimetics identified stimulate GLUT4 translocation by a mechanism that is independent of the presence of the hInsR.

CONCLUSIONS AND IMPLICATIONS

Taken together, the results indicate that TIRF microscopy is an excellent tool for the quantification of GLUT4 translocation and for identifying insulin mimetic drugs.

Abbreviations

2-DG, 2-deoxyglucose; ABA, abscisic acid; AFM, atomic force microscopy; BBR, berberine; BI, bilberry; GA, gallic acid; GE, guava; GLUT4, glucose transporter 4; GSC, GLUT4 storage compartments; GS, grape skin; hInsR, human insulin receptor; KRPH, Krebs-Ringer phosphate HEPES; PCR, purple carrot red; RC, red cabbage; SP, sweet potato; TA, tannic acid; TIRF, total internal reflection fluorescence

© 2014 The Authors. British Journal of Pharmacology published by John Wiley & Sons Ltd on behalf of The British Pharmacological Society.
This is an open access article under the terms of the Creative Commons Attribution-NonCommercial-NoDerivs License, which permits use and distribution in any medium, provided the original work is properly cited, the use is non-commercial and no modifications or adaptations are made.

Table of Links

TARGETS	LIGANDS
EGFR	2-DG
GLUT4	Insulin
GPR35	NADPH
InsR	PIP_3
SERT (5-HT transporter)	Tannic acid
SGLT1	Wortmannin

This Table lists key protein targets and ligands in this document, which are hyperlinked to corresponding entries in http://www.guidetopharmacology.org, the common portal for data from the IUPHAR/BPS Guide to PHARMACOLOGY (Pawson *et al.*, 2014) and are permanently archived in the Concise Guide to PHARMACOLOGY 2013/14 (Alexander *et al.*, 2013a,b,c).

Introduction

Insulin promotes the uptake of glucose by adipocytes and muscle cells through glucose transporter 4 (GLUT4). This glucose flux is a tightly controlled process and has a key role in the reduction of blood glucose levels and hence is of particular importance in diabetes (Pessin and Saltiel, 2000; Kahn *et al.*, 2006; Klip, 2009). In unstimulated cells, GLUT4 is mainly (more than 90%) stored in perinuclear regions, termed GLUT4 storage compartments (GSC; Bryant *et al.*, 2002; Stockli *et al.*, 2011), resulting in low basal glucose flux. Insulin stimulation induces the redistribution of GLUT4 to the plasma membrane (Figure 1A). In the past few years, a huge effort has been made to identify substances, termed insulin mimetic drugs, which increase the GLUT4 translocation to the plasma membrane independently of insulin. However, up to now, a major breakthrough in finding a substance that selectively enhances glucose uptake could not be achieved in pharmaceutical research. An explanation for this failure might lie in the low availability of efficient, quantitative and simple *in vitro* systems and assays that can be used to investigate GLUT4 translocation. In many cases, experi-

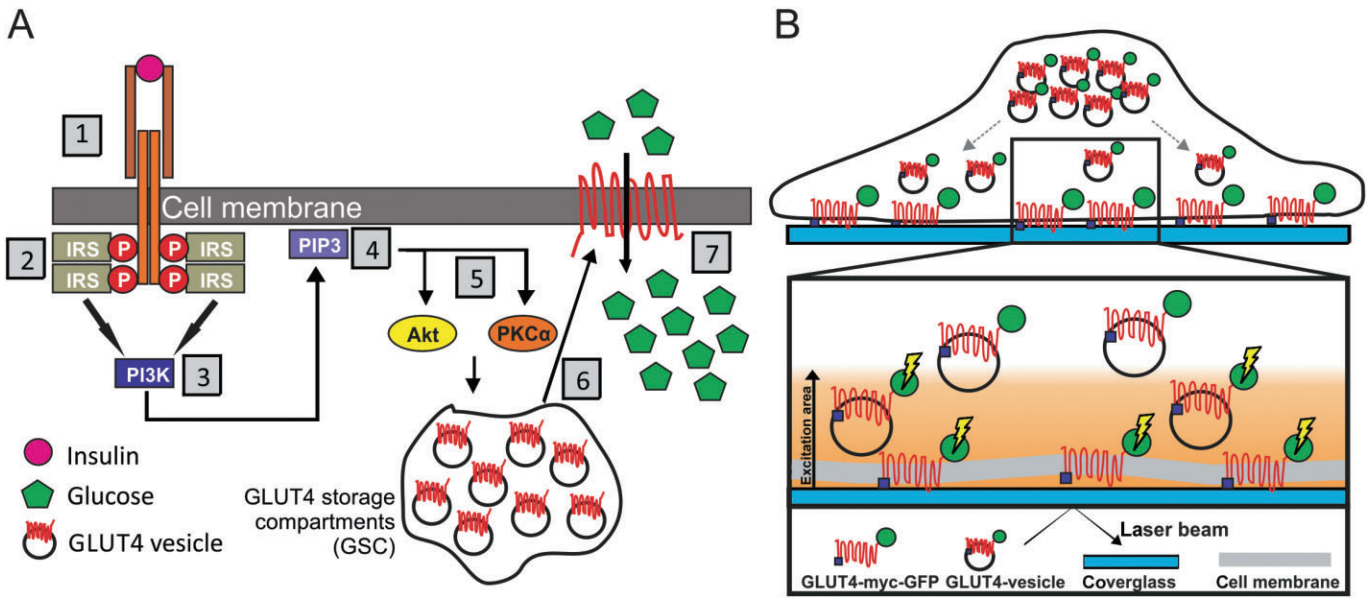

Figure 1

Schematic diagram of insulin-mediated GLUT4 translocation and analysis by TIRF microscopy. (A) Key signal transduction events of GLUT4 translocation. Binding of insulin to its receptor (1) induces autophosphorylation, recruitment of insulin receptor substrate (IRS) proteins (2) and activation of PI3K (3). Formation of PIP_3 (4) leads to the activation of Akt and PKCα (5) followed by translocation of GLUT4-containing vesicles from intracellular compartments (6) to the plasma membrane. Insertion of GLUT4 into the plasma membrane finally triggers the uptake of glucose (7). (B) Schematic model of TIRF microscopy to measure GLUT4 accumulation in the evanescent field. Cells expressing GLUT4-myc-GFP are grown in TIRF microscopy-compatible (coverslip glass) 96-well microplates. Only fluorophores localized to the TIRF zone are excited (~150–200 nm penetration depth).

ments are based on indirect wet-lab approaches including Western blot analysis of membrane fractions, ELISA-guided binding assays and flow cytometric analysis (Kristiansen and Richter, 2002; Bruzzone *et al.*, 2012; Kadan *et al.*, 2013). Furthermore, microscopy-guided approaches including immunoelectron techniques have been used (Carvalho *et al.*, 2004). However, most of the aforementioned methods suffer from being indirect, time consuming, non-quantitative, not sensitive enough and/or are very expensive.

An important improvement for investigations into cellular GLUT4 localization was the insertion of different epitope tags (mainly myc and HA) in the first extracellular loop of the GLUT4 protein in combination with a genetically encoded fluorophore (mainly GFP) at the c-terminal end of the transporter (Jiang *et al.*, 2002; Baus *et al.*, 2008). Confocal fluorescence microscopy has been successfully used to characterize the transport of GLUT4-containing vesicles from perinuclear regions to and the insertion of the transporter into the plasma membrane using such chimeric fusion proteins (Lampson *et al.*, 2000; Baus *et al.*, 2008; Liu *et al.*, 2009). Unfortunately, most cellular glucose uptake models are hard to transfect, and some of these cells need to be differentiated, which is time consuming. Recently, a CHO-K1 cell line stably expressing the human insulin receptor (hInsR) and a GLUT4-myc-GFP construct has been introduced (Vijayakumar *et al.*, 2010). These cells do not need to be differentiated, are highly sensitive to insulin and, by applying confocal microscopy, were used to characterize the effect of an insulin mimetic, fenugreek seeds extract (Vijayakumar *et al.*, 2010; Vijayakumar and Bhat, 2012).

Total internal reflection fluorescence (TIRF) microscopy has become a method of choice to investigate GLUT4 trafficking, allowing for the selective capture of the docking and fusion events that take place adjacent to the plasma membrane (Lampson *et al.*, 2001; Bai *et al.*, 2007; Xiong *et al.*, 2010). In addition, this microscopy technique has served as a powerful tool to identify key players involved in the trafficking of GLUT4. For example, multiple Rab proteins were found to regulate the final steps of insulin-stimulated translocation to the plasma membrane in adipocytes (Chen *et al.*, 2012). However, while the importance of TIRF microscopy to obtain insights into the GLUT4 translocation machinery is inconceivable, its potential as a method for quantifying GLUT4 translocation at competitive throughput rates has not been implemented so far. As there is a huge demand for insulin mimetics for better treatments or the prevention of type 2 diabetes, such a screening method would be extremely helpful. Globally, as of 2010, it was estimated that there were 285 million people with type 2 diabetes (Smyth and Heron, 2006), which is caused by a combination of insulin resistance and inadequate compensatory insulin secretion (Creager *et al.*, 2003). Thus, the identification of substances that bypass the lack of functional insulin receptors to induce GLUT4 translocation is of tremendous importance.

Here we present a study implementing dual-colour TIRF microscopy to detect and quantify GLUT4 translocation in a CHO-K1 cell line overexpressing the hInsR and a GLUT4-myc-GFP fusion protein introduced by Vijayakumar and co-workers (Vijayakumar *et al.*, 2010). We quantified the GLUT4 signal in the evanescent field under serum-free (starvation) or stimulated conditions in the presence of different GLUT4 translocation modulators. We compared the fluorescence of the GFP signal in live and fixed cells to the one of labelled antibodies targeting the exofacial loop of the GLUT4 molecule, and proved the suitability of the method to generate simple dose–response relationships. The increase in the GLUT4-GFP signal induced on stimulation was correlated with intracellular glucose levels using a 2-deoxyglucose (2-DG) based uptake assay. In addition, we correlated the epi-fluorescence with atomic force microscopy (AFM) studies and confirmed a significant increase in the GLUT4 fraction inserted in the membrane upon insulin stimulation. We utilized our assay to identify novel substances that function as insulin mimetics. For our analysis, we developed appropiate software, which enabled rapid quantification of the fluorescence signal. Our studies clearly show that TIRF microscopy is an excellent technology for the better characterization of known, and the identification of new insulin mimetic drugs.

Methods

DNA constructs and chemicals

The pcDNA3-GLUT4-myc-GFP was kindly provided by J. E. Pessin (Albert Einstein College of Medicine, New York). Glucose Uptake Colorimetric Assay Kit, human insulin, wortmannin, HEPES, $CaCl_2$, NaCl, KCl, $MgSO_4$, KH_2PO_4, LY294,002, abscisic acid (ABA), tannic acid (TA), chlorogenic acid, gallic acid (GA) and berberine (BBR) were purchased from Sigma-Aldrich (Schnelldorf, Germany). Mouse anti-myc monoclonal antibody (9E10: sc-40 and sc-40 AF647) was from Santa Cruz Biotechnology (Santa Cruz, CA, USA) and rabbit anti-insulin receptor α (Alexa 647) was purchased from antibodies-online (Aachen, Germany). Sea-buckthorn juice was a gift from Anton Hübner GmbH (Ehrenkirchen, Germany). Red cabbage (RC), sweet potato (SP), purple carrot red (PCR), bilberry (BI), grape skin (GS) and guava (GE) extracts were provided by Belan GmbH (Wels, Austria).

Cell culture and transfection

CHO-K1 cells stably expressing hInsR and GLUT4-myc-GFP were a kind gift from Manoj K. Bhat (National Centre for Cell Science, University of Pune, India). CHO-K1 hInsR-GLUT4-myc-GFP, CHO-K1 GPI-GFP, CHO-K1 CD147-YFP and CHO-K1 EGFR-GFP cells were maintained in Ham's F12 culture medium supplemented with 100 $\mu g \cdot mL^{-1}$ penicillin, 100 $\mu g \cdot L^{-1}$ streptomycin, 1% G418 and 10% FBS (all Life Technologies, Carlsbad, CA, USA), and grown in a humidified atmosphere at 37°C and 5% CO_2. A stable clone of CHO-K1 GLUT4-myc-GFP cells was generated using electroporation, briefly, the day before transfection CHO-K1 (DSMZ, Braunschweig, Germany) cells were subcultured and transfected the day after at 50–70% confluence with 1–5 μg DNA using the Nucleofector device. For transfection DMEM/Ham's F12 without FBS and penicillin/streptomycin was used. Cells were plated into 60 mm culture dishes and grown for 48 h. The medium was removed and replaced with fresh medium supplemented with 400 $\mu g \cdot mL^{-1}$ G418. The medium was changed every 3 days and 15–20 days later individual neomycin-resistant colonies were selected for propagation and analysis. CHO-K1 GLUT4-myc-GFP cells were

maintained in DMEM/Ham's F12 culture medium supplemented with 100 $\mu g \cdot mL^{-1}$ penicillin, 100 $\mu g \cdot L^{-1}$ streptomycin, 1% G418 and 10% FBS (all Life Technologies), and grown in a humidified atmosphere at 37°C and 5% CO_2.

TIRF microscopy

For microscopy experiments cells were grown in 96-well imaging plates (50 000 cells·per well; Nunc, Roskilde, Denmark) overnight. Cell culture medium was aspirated off and, after the cells had been washed with PBS (VWR, Vienna, Austria), replaced by HBSS (PAA Laboratories, Pasching, Austria), supplemented with 0.1% BSA (Sigma-Aldrich) for 3–4 h. Cells were then treated with indicated substances dissolved in Krebs-Ringer phosphate HEPES buffer (KRPH; 20 mM HEPES, 1 mM $CaCl_2$, 136 mM NaCl, 4.7 mM KCl, 1 mM $MgSO_4$ and 5 mM KH_2PO_4) or HBSS buffer and imaged on an Olympus IX-81 inverted microscope (Olympus, Tokyo, Japan) in objective-type TIR configuration via an Olympus 60× NA = 1.49 Plan-Apochromat objective. 96-well plates were placed on a x-y-stage (CMR-STG-MHIX2-motorized table; Märzhäuser, Wetzlar, Germany). Scanning of larger areas was supported by a laser-guided automated focus-hold system (ZDC2). This system provided by Olympus uses a non-destructive IR laser to continuously maintain the sample position and focus for a short or long term time-lapse imaging. Thus, changes caused by varying temperatures or the addition of reagents, can be compensated for. The 488 and 647 nm emissions of diode lasers (Toptica Photonics, Munich, Germany) were used to image GFP and Alexa647 fluorescence respectively. After appropriate filtering, the fluorescence signal was recorded via an Orca-R2 CCD camera (Hamamatsu Photonics, Herrsching, Germany).

Immunofluorescence

Cells grown in 96-well imaging plates were deprived of serum (starved) and incubated with insulin or GLUT4 translocation-modifying reagents. Afterwards, the cells were fixed with 4% pre-cooled paraformaldehyde (Sigma-Aldrich) for 15 min on ice followed by two washing steps with PBS and a blocking step with 5% FBS and 5% BSA in PBS for 1 h at 4°C. The blocking solution was replaced by 4 $\mu g \cdot mL^{-1}$ anti-myc Alexa647 antibody diluted in PBS for 1 h. Before the microscopy experiments, three additional PBS washing steps were carried out.

Correlation of epi-fluorescence with AFM force measurements

CHO-K1 GLUT4-myc-GFP hInsR cells were grown on standard 30 mm glass slides (VWR) overnight. Cell culture medium was aspirated off and, after the cells had been washed with PBS, replaced by HBSS supplemented with 0.1% BSA for 3–4 h. Cells were then treated with 100 nM insulin dissolved in KRPH buffer for 10 min and fixed by addition of 4% pre-cooled paraformaldehyde for 10 min on ice followed by two washing steps with PBS. For AFM force measurements, the anti-myc antibody was firstly purified using a PD10 column (GE Healthcare, Buckinghamshire, UK) eluted in PBS and finally was covalently bound onto AFM tips (MSCT, Bruker, Billerica, MA, USA) via a home-made flexible heterobifunctional polyethylene glycol (PEG) linker, NHS-PEG_{18}-acetal, as described previously (Wildling *et al.*, 2011). Further fluorescence-guided AFM studies were performed on a 6000 ILM AFM set-up (Agilent Technologies Inc., Chandler, AZ, USA) integrated with an inverted optical microscope Zeiss Observer.D1 (Zeiss, Oberkochen, Germany). Firstly, phase contrast/fluorescent images were obtained using a 20× objective (Zeiss) and captured by a digital camera ORCA-Flash 2.8 (Hamamatsu Photonics, Hamamatsu, Japan). Fluorescence images were acquired using an Oligochrome light source lamp (Till Photonics, Gräfelfing, Germany) and EGFP HC filter set (Semrock Inc., Rochester, NY, USA). AFM force-distance cycles were then collected on a cell of interest using an antibody-functionalized cantilever with a nominal spring constant of 20 $pN \cdot nm^{-1}$ (Figure 3D). For each cell preparation (either deprived of serum or insulin stimulated), at least three different cells expressing GLUT4 receptors were tested with three different AFM cantilevers. Each AFM/fluorescence experiment was obtained at least in duplicate using independent cell preparations. Finally, the binding probabilities (probability to record an unbinding event in one force-distance cycle) from several experiments were quantified.

2-DG uptake assay

Glucose uptake experiments were conducted according to manufacturer's instructions. In this assay, 2-DG uptake is determined by a coupled enzymatic reaction in which 2-DG6P is oxidized, resulting in the generation of NADPH. NADPH is further processed to TNB, which can be detected at 412 nm. In short, CHO-K1 GLUT4-myc-GFP cells were plated at 5×10^4 cells per well the night before the experiment in 96-well plates. The medium was replaced by HBSS for 3–4 h followed by 1 h incubation in KRPH buffer (20 mM HEPES, 5 mM KH_2PO_4, 1 mM $MgSO_4$, 1 mM $CaCl_2$, 136 mM NaCl and 4.7 mM KCl, pH 7.4). Cells were then stimulated with the indicated drugs (100 µL·per well) for 40 min and 10 µL of 10 mM 2-DG was added for a further 20 min. Cells were washed three times with PBS, lysed with 80 µL of extraction buffer, freeze/thawed in liquid nitrogen and heated at 85°C for 40 min. The lysates were cooled down on ice for 5 min and neutralized by adding 10 µL of neutralization buffer. Insoluble material was removed by spinning down the extract at 21.300 rcf for 5 min and the lysate was then diluted 1:10 in assay buffer. Finally, TNB generation was set up by two amplification steps according to instructions. Absorbance was measured at 412 nm on a plate reader (POLARstar omega, BMG LABTECH, Ortenberg, Germany). Each sample was measured in duplicate.

Data analysis

Initial imaging recordings were supported by the Olympus Xcellence RT software. In-depth analysis for the calculation of the fluorescence intensity in individual cells and a fast comparison of the fluorescent signal in numerous cells at different time intervals was performed using the Spotty framework (Spotty can be retrieved online at http://bioinformatics.fh-hagenberg.at/projects/microprot/). The most important analysis algorithms integrated in the intensity analysis in Spotty are (i) pre-processing (including correlation based optimal downsampling, filtering and creation of layer-based images), (ii) cell detection and (iii) results analysis. Statistical analysis was carried out using Graphpad Prism (GraphPad Software, La Jolla, CA, USA).

Results

TIRF microscopy-guided analysis of GLUT4 translocation

We used TIRF microscopy to detect and quantify GLUT4 translocation in CHO-K1 cells overexpressing the hInsR together with a GLUT4-myc-GFP fusion protein (Vijayakumar and Bhat, 2012; Figure 1B). The development of a TIRF microscopy-based screening system for insulin-modifying substances provides a simple and fast analysis of the GLUT4 signal. This procedure excludes the use of fixed cells in combination with fluorescent antibodies.

Importantly, our experimental settings including the stable GLUT4-myc-GFP/hInsR expressing clone, fast high-precision scanning microscopy and TIRF-compatible 96-well plates generate large amounts of data, which can only be handled by the use of appropriate software. To address this, we developed an algorithm that allows for fast and automated analysis of recorded data. Key features of the programme, which was originally developed for the quantification of protein–protein interactions (Lanzerstorfer *et al.*, 2013), include (i) an automated (or manual) detection of fluorescent cells; (ii) quantification of the respective fluorescence signal; (iii) the ability to simultaneously analyse selected areas in several images; (iv) an automated calculation of changes in the fluorescent signal induced by GLUT4 translocation-modifying substances; and (v) an export function of the raw data obtained. This programme, which can be retrieved online as described in the Methods section, was used for quantification of all the data presented in this study.

In a first attempt, we only determined the intensity of the GFP signal. These experiments could be carried out in live cells and enabled the analysis of the GLUT4 fluorescence within the same cell subjected to 'starvation' conditions and after being stimulated with insulin. As shown in Figure 2, addition of 17 μM insulin (this concentration was found to induce a maximum response in this cell line) significantly increased the fluorescence signal by ~80% within 10 min and ~200% within 60 min, respectively, compared with the non-induced condition. Pre-incubation with 1 μM of the PI3K inhibitor wortmannin (Clarke *et al.*, 1994) for 60 min effectively reduced this GLUT4 signal increase. In addition, we observed an increase in the GLUT4 signal, of about 25% within 10 min, when the 'starvation' buffer was replaced by fresh HBSS buffer (mock control). No further increase could be detected after a one hour incubation under these conditions. This increase in GLUT4 translocation in the absence of

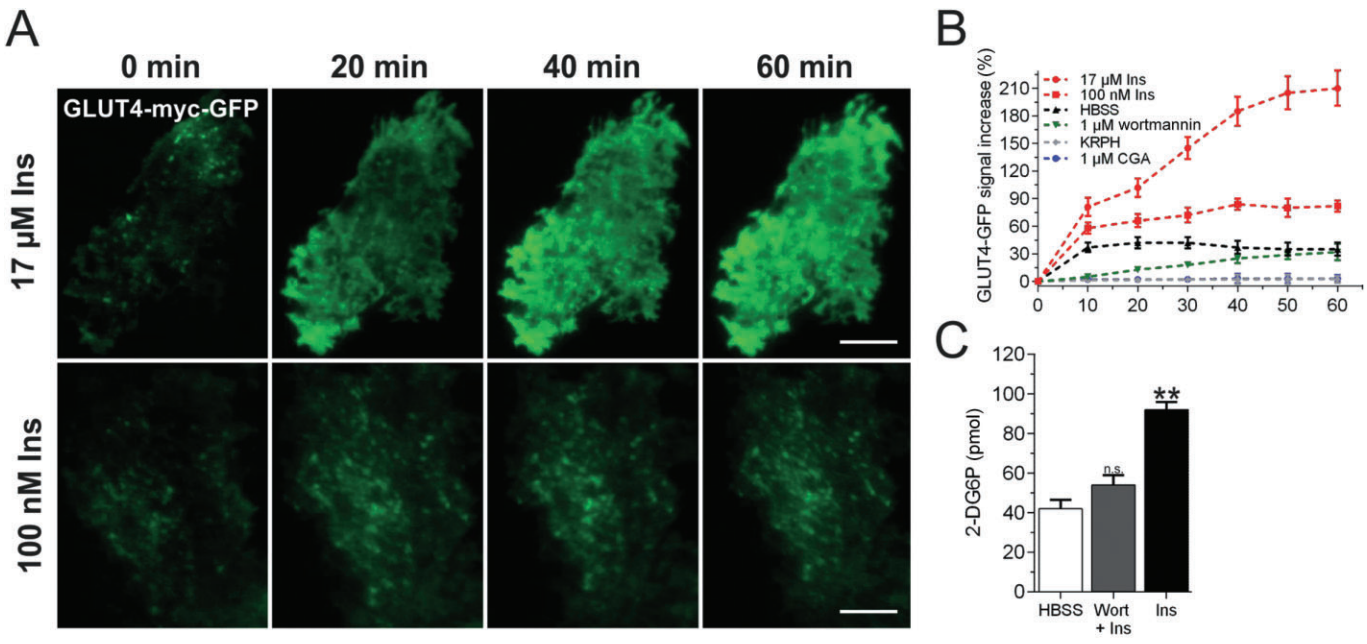

Figure 2

Quantification of GLUT4 translocation by live-cell TIRF microscopy. (A) Representative TIRF images (488 nm excitation) of CHO-K1 hInsR/GLUT4-myc-GFP. Cells were seeded in 96-well plates (50 000 cells·per well) and grown overnight followed by 3–4 h of starvation in HBSS buffer. Stimulation by insulin (17 μM and 100 nM, respectively) led to a significant increase in the fluorescence intensity within 60 min. Scale bar = 7 μm. (B) Temporal resolution of the change in GFP fluorescence intensity in the evanescent field. Images were captured after addition of 100 nM insulin, 17 μM insulin or 17 μM insulin + 1 μM wortmannin respectively. HBSS and KRPH buffer exchange served as mock control; 1 μM chlorogenic acid was dissolved in KRPH buffer. Fluorescence was normalized to the value before insulin application. Error bars are based on the SEM. At least 200 cells were analysed for each condition. Data were collected from the same cells before and after drug application. (C) 2-DG glucose uptake assay. CHO-K1 GLUT4-myc-GFP cells were grown in 96-well plates and starved for 3–4 h in HBSS buffer followed by glucose deprivation in Krebs-Ringer buffer for 1 h. Cells were then stimulated by 17 μM insulin in the absence or presence of 1 μM wortmannin for 1 h followed by addition of 2-DG (20 min). Cell extracts were prepared and 2-DG uptake was measured after a colorimetric reaction using a plate reader device. Samples were measured in duplicates. Error bars are based on SEM. $^{**}P < 0.01$, significant increase with respect to HBSS and wortmannin control.

insulin is in line with other studies for which biochemical glucose uptake assays have been performed (Jung *et al.*, 2011), and is mainly caused by unconsumed glucose present in the HBSS buffer. When KRPH buffer that lacks glucose was used instead of HBSS no increase in GLUT4 fluorescence could be detected. The effects of different 'starvation' conditions can be found in Supporting Information Fig. S1. Starvation in HBSS buffer reduced the fluorescence intensity of the GFP signal in the evanescent field significantly more than starvation in medium lacking serum. Accordingly, the insulin sensitivity was much higher in HBSS starved cells.

We also determined the change in the GLUT4 signal in response to 100 nM insulin. Under these conditions, we found a fast increase of ~60% within 10 and ~75% within 60 min. Many substances that were tested did not lead to an increase in the GFP signal. As an example the response to the polyphenolic compound chlorogenic acid (dissolved in KRPH buffer) is shown in Figure 2B.

As a control, we determined whether insulin strengthens the adhesion of the cells to surface and thus leads to a false-positive increase in the TIRF signal. For this purpose, CHO-K1 cells expressing the plasma membrane-localized proteins CD147-GFP, GPI-anchored GFP or EGFR-GFP (Weghuber *et al.*, 2011; Lanzerstorfer *et al.*, 2014) were treated with insulin and the respective fluorescence signal in TIRF configuration was recorded within 1 h post-stimulation. As shown in Supporting Information Fig. S2, no significant changes in the fluorescence intensity were found.

Correlation of intracellular glucose levels with GLUT4-GFP fluorescence

An ultimate control, which confirms that the increase in the GFP signal in the evanescent field is really caused by an elevated insertion of the functional transporter into the plasma membrane, is the determination of intracellular glucose levels. We used a 2-DG-based glucose uptake assay to quantify the glucose concentration of starved, stimulated and/or wortmannin-treated CHO-K1 expressing GLUT4-myc-GFP. As indicated in Figure 2C, we found about 40 pmol 2-DG6P in cells starved in HBSS buffer. The concentration increased to ~95 pmol upon insulin stimulation. Wortmannin pre-incubation (1 μM for 60 min) effectively inhibited the stimulating effect of insulin. In conclusion, the GLUT4 signal increase observed by TIRF microscopy is closely associated with elevated glucose concentrations within these cells.

Increased GLUT4-GFP fluorescence as a direct parameter for stimulated GLUT4 translocation

In addition to the glucose uptake assay, we used the myc tag in the first exofacial loop of the GLUT4 protein to prove that an increasing GFP signal is really due to an elevated insertion of the transporter into the plasma membrane. The myc tag enables the detection of molecules, which are exclusively inserted into the plasma membrane (Jiang *et al.*, 2002). We used this tag in order to compare the GLUT4 translocation in live and fixed cells, and to confirm that the observed increase in the GFP signal is closely correlated with an elevated myc signal.

Therefore, we starved CHO-K1-hInsR-GLUT4-myc-GFP cells for 4 h in HBSS buffer, induced GLUT4 translocation by insulin, fixed the cells with paraformaldehyde and labelled them with an anti-myc Alexa647 antibody. It is generally accepted that the basal membrane of adherent cells is easily accessible to antibody binding: the distance between the cell and its substrate has been found to be great enough to ensure sufficient distribution and proper binding of antibodies (Giebel *et al.*, 1999). TIRF microscopy was used to quantify the fluorescence in both colour channels. In this case, cell fixation is a prerequisite if antibodies are used to immunostain the respective target. Naturally, the fixation process precludes the comparison of the fluorescence intensity before and after addition of insulin in the same cell. At the same time, the GLUT4-myc-GFP expression rates vary markedly between individual cells, rendering the comparison of differently treated samples more complicated. To circumvent these limitations, we quantifed the fluorescence intensity of $n > 500$ cells for each sample. Figure 3A depicts representative images of starved and insulin-treated cells in both colour channels. As shown in Figure 3B, we detected an increase in the GFP fluorescence upon insulin stimulation (100 nM for 10 min) of 1.6-fold, which is identical to the one described for live cells (Figure 2B). The fluorescent intensity of cells

Figure 3

The increase in the GFP signal and myc staining upon insulin stimulation. (A) Representative TIRF microscopy images of GLUT4-GFP and Alexa647-anti-myc staining under basal and insulin-stimulated (100 nM, 10 min) conditions. CHO-K1 hInsR/GLUT4-myc-GFP cells were grown overnight in 96-well plates (50 000 cells·per well) and then starved for 3–4 h in HBSS buffer. Cells were fixed with 4% paraformaldehyde and stained using an Alexa647 labelled anti-myc antibody. Fluorescence in the evanescent field was recorded for GFP and Alexa647 at 488 and 640 nm respectively. Scale bar = 10 μm. (B) Quantification of respective fluorescence signals in starved and insulin-treated cells ($n > 200$ cells). Fluorescence was normalized to the values before stimulation. Error bars are based on the SEM. $^*P < 0.05$ and $^{**}P < 0.01$, significant increase with respect to starved cells respectively. (C) Fluorescence intensity profiles for the indicated line scans (marked in yellow in A) of a representative starved and insulin-stimulated cell respectively. (D) Fluorescence-guided AFM force measurements on CHO-K1 GLUT4-myc-GFP hInsR cells. (E) By overlapping phase contrast and fluorescence images, it was possible to visualize the AFM cantilever and thus to guide it onto a cell of interest. (F) AFM tip/cantilever assembly approaches and retracts from the cellular surface, and the deflection of the tip is recorded. As the AFM tip decorated with an anti-myc antibody approaches the cell surface (approach curve in red), a specific antibody-receptor bond can be created. Retraction of the tip from the cell surface leads to linker/bond stretching, and at a critical moment the bond will be ruptured (represented as an unbinding event). Two typical force-distance cycles recorded on GLUT4-myc-GFP-positive cells are shown: one retrace curve (in blue) illustrates a specific interaction event, whereas another one (light blue) does not contain unbinding events. (G) Binding probability of starved and insulin-treated (100 nM for 10 min) CHO-K1 GLUT4-myc-GFP hInsR cells. Error bars are based on the SEM. $^{**}P < 0.01$, significant increase with respect to starved cells. Lowest and highest values of each data set were taken as 0 and 100% response for normalization respectively.

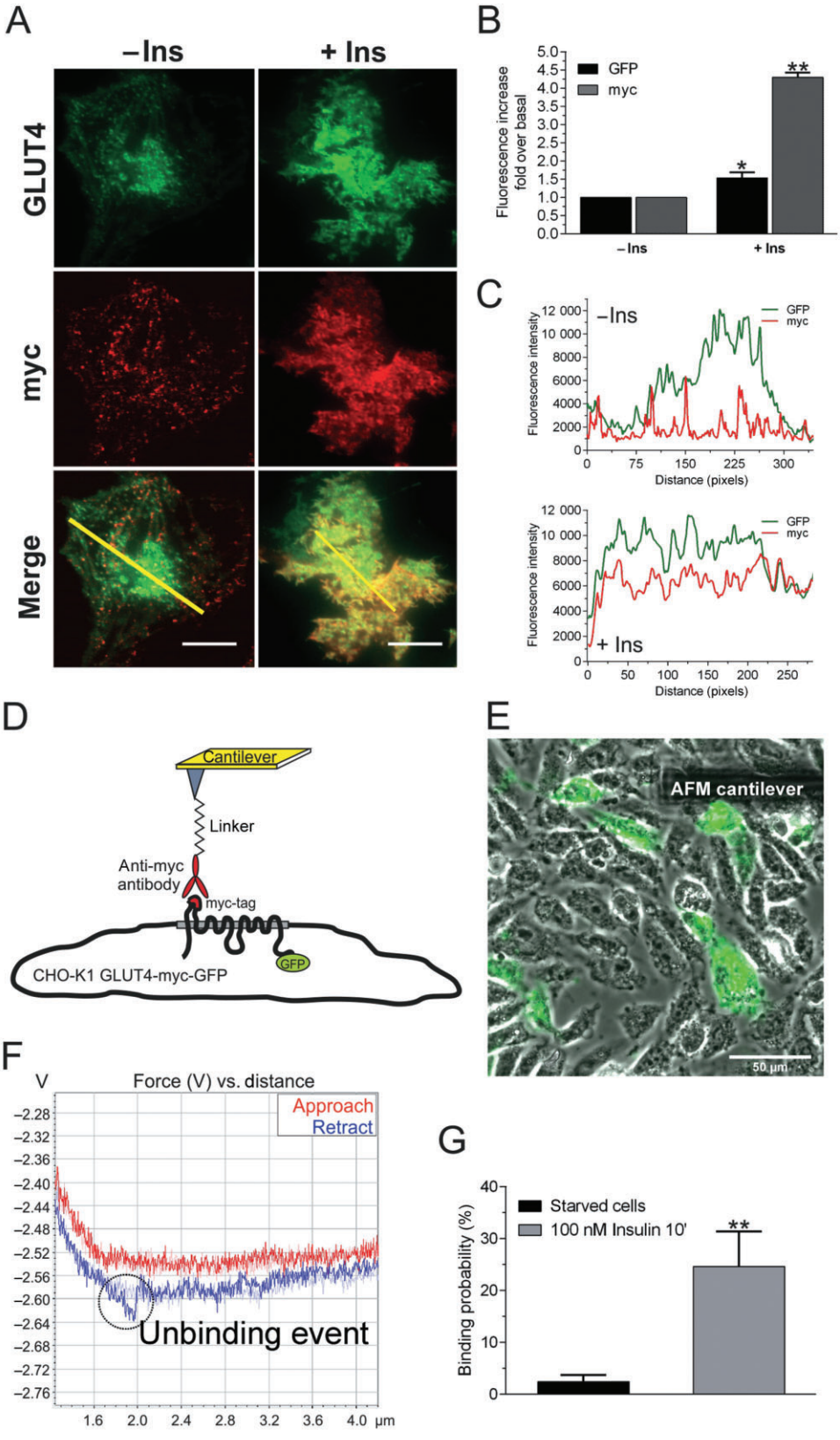
A
–Ins
+ Ins
GLUT4
myc
Merge
B
Fluorescence increase fold over basal
GFP
myc
–Ins
+ Ins
C
–Ins
+ Ins
Fluorescence intensity
Distance (pixels)
D
Cantilever
Linker
Anti-myc antibody
myc-tag
GFP
CHO-K1 GLUT4-myc-GFP
E
AFM cantilever
50 µm
F
Force (V) vs. distance
Approach
Retract
Unbinding event
G
Starved cells
100 nM Insulin 10'
Binding probability (%)

stained by the Alexa647 labelled anti-myc antibody was increased approximately fourfold. The higher percentage increase of the myc signal was due to the much lower background in the myc channel under starvation conditions compared with the GFP signal. We determined the co-localization of GFP and the myc tag fluorescence at a single-cell level by line scan analysis (Figure 3C): while the co-localization of both signals was evident in stimulated cells (Pearson's coefficient GFP-myc = 0.33), the degree of co-localization was low under starvation conditions (GFP-myc = 0.01). In conclusion, an increase in GFP fluorescence was found to correlate well with elevated staining of the extracellular myc tag.

AFM force spectroscopy experiments confirm the increased GLUT4 translocation

In addition to the quantification of the GFP/myc signals and the analysis of changes in intracellular glucose concentrations, fluorescence-guided AFM force measurements were performed to detect GLUT4-myc-GFP molecules on the surface of CHO-K1 hInsR cells under starvation and insulin-stimulated conditions. These control experiments are reasonable since the fixation procedure required for the myc staining might slightly permeabilize the cells and thus lead to staining of intracellular GLUT4 molecules as well. AFM has been successfully used to study receptor–ligand interactions at the single-molecule level with transmembrane transporters such as SGLT1 (sodium glucose transporter 1; Puntheeranurak *et al.*, 2006) and the 5-HT transporter (Wildling *et al.*, 2012) on living cells, and to localize various membrane receptor molecules on cellular surfaces (Chtcheglova *et al.*, 2008; 2010). For our experiments, an anti-myc antibody was bound to the AFM tip (Figure 3D) to unequivocally detect GLUT4-myc-GFP on the surface of the cells. Naturally, the fixation process, which is needed for the sample preparation, is of no consequence since the antibody is covalently coupled to the cantilever. Thus, only the complete membrane-inserted fraction of GLUT4 can be detected.

On CHO-K1 GLUT4-myc-GFP hInsR cells, a series of specific binding events were observed (see Figure 3E and F). From several hundreds of force-distance cycles, one can determine the binding probability. A significant difference between starved and insulin-treated cells was observed (Figure 3G): only a few unbinding events (e.g. specific unbinding of anti-myc antibody from GLUT4-myc proteins on the cellular surface) could be detected on the starved cells (2.4 ± 1.3% binding probability), the number of unbinding events was significantly increased on the stimulated cells (24.6 ± 6.8% binding probability). Taken together, the observed effect of the GFP signal was found to correlate with the elevated myc staining rates, unbinding events and intracellular glucose levels. Thus, analysis of the GFP signal is a suitable parameter for detecting and estimating GLUT4 insertion into the plasma membrane.

Stimulation and inhibition of GLUT4 translocation quantified by TIRF microscopy

We continued our work by analysing the effects of various insulin concentrations on the GLUT4-GFP signal in the evanescent field. In these experiments, we analysed the fluorescence within the same live cells before and after addition of insulin and quantified the fluorescent signal of $n > 500$ cells for each concentration. As expected, we found an insulin concentration-dependent increase in the GLUT4-GFP signal: incubation with 0.1 nM, 1 nM, 10 nM, 100 nM, 850 nM, 1.7 μM, 17 μM and 170 μM insulin for 60 min resulted in a characteristic dose–response relationship as shown in Figure 4A. The EC_{50} value was estimated as 1.7 μM.

In the next set of experiments, we studied the effects of different inhibitors on GLUT4 translocation. First, we tested the PI3K inhibitor wortmannin in live cells. For these experiments, the cells were pretreated with different wortmannin concentrations (1 nM, 10 nM, 20 nM, 50 nM, 100 nM, 316 nM, 1 μM) for 60 min in medium containing serum. We then quantified the GFP signal of $n > 200$ cells for each

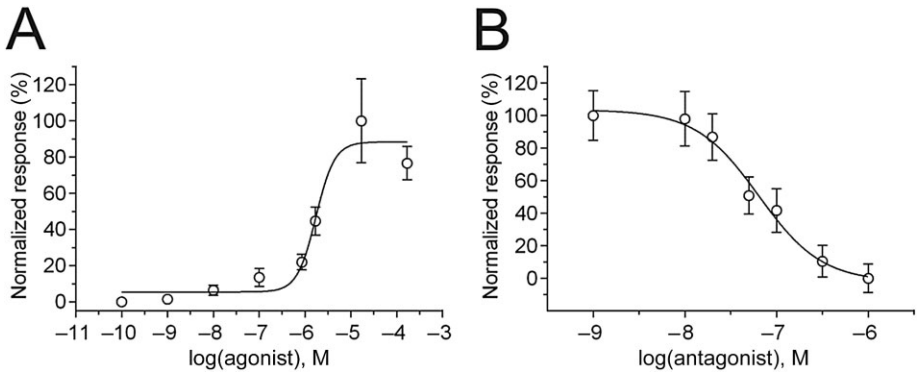

Figure 4

Insulin and wortmannin sensitivity of GLUT4 translocation. (A) CHO-K1 hInsR/GLUT4-myc-GFP cells were seeded in 96-well plates (50 000 cells·per well), grown overnight and then starved for 3–4 h in HBSS buffer followed by addition of various insulin concentrations (1 h incubation time). A normalized dose–response curve was generated by measuring the increase in the GFP signal in the evanescent field (488 nm excitation) after application of the indicated insulin concentrations. (B) CHO-K1 hInsR/GLUT4-myc-GFP cells were seeded in 96-well plates in medium including serum. A normalized dose–response curve was generated by measuring the GFP signal after treatment with the indicated wortmannin concentration (1 h incubation time). At least 200 cells were analysed for each concentration. Error bars are based on the SEM.

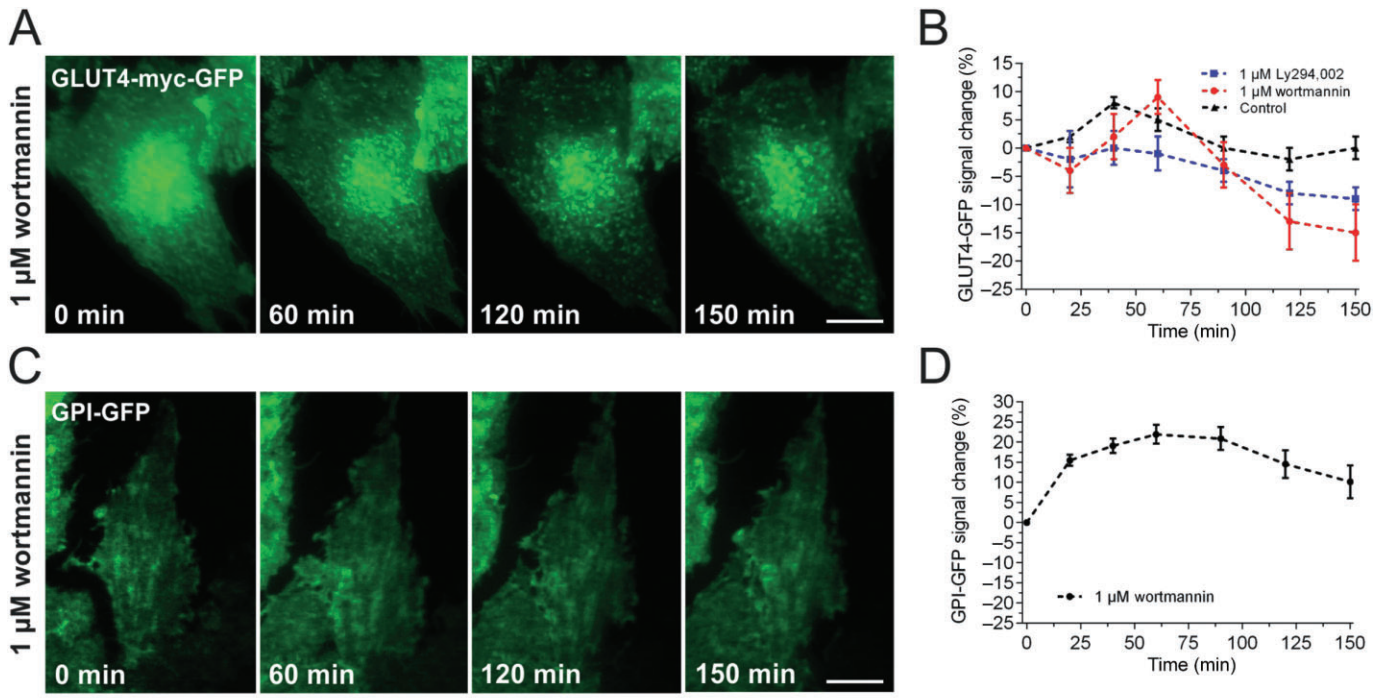

Figure 5

Temporal resolution of GLUT4 translocation inhibitors. (A) Representative TIRF microscopy images (488 nm excitation) of wortmannin-treated (1 µM) CHO-K1 hInsR/GLUT4-myc-GFP cells at the indicated time points. Scale bar = 7 µm. (B) Time course of the decrease in the fluorescence intensity within 150 min after addition of the indicated substance. CHO-K1 hInsR/GLUT4-myc-GFP cells were seeded in 96-well plates (50 000 cells·per well) and grown overnight in medium including serum followed by addition of the indicated substance. Medium including serum served as a control. Fluorescence was normalized to the value before application of the inhibitor ($n > 100$ cells). Data were collected from the same cells before and after drug application. Error bars are based on the SEM. (C) Representative TIRF microscopy images of wortmannin-treated (1 µM) CHO-GPI-GFP cells at the indicated time points. Scale bar = 7 µm. (D) Quantification of the change in fluorescence intensity of GPI-GFP within 150 min after wortmannin application. CHO-K1-GPI-GFP cells were seeded in 96-well plates (50 000 cells·per well) and grown overnight followed by addition of the indicated substance. Fluorescence was normalized to the value before inhibitor addition ($n > 200$ cells).

sample. As indicated in Figure 4B, an increasing wortmannin concentration resulted in significantly reduced fluorescence intensity. Based on the respective dose–response relationship, the IC_{50} value was calculated as 6.4 nM.

In addition, we investigated the effects of the GLUT4 translocation inhibitor LY294,002 in comparison with wortmannin. LY294,002 is a known inhibitor of PI3K, but somewhat less potent than wortmannin (Maira *et al.*, 2009). For these experiments, we determined the extent of the GFP signal decrease in the same live cells (grown in medium including serum) after drug application (Figure 5A). As shown in Figure 5B, the fluorescence dropped by 10% within 150 min post-LY294,002 addition, while no decrease was observed when the incubation medium was replaced by fresh, serum-containing medium. Our experiments also confirmed a reduced efficacy of LY294,002 in comparison to wortmannin, which decreased the GLUT4 signal by 15% within the same time period. To exclude a potential weakening of cell adhesion upon wortmannin treatment, which would result in a misleading decrease in the TIRF signal, we determined the fluorescence of a plasma membrane localized protein that should not be affected by the addition of wortmannin. Therefore, we treated CHO-K1 cells stably expressing a GPI-anchored GFP with wortmannin and recorded the fluorescence in TIRF configuration over 150 min. As shown in Figure 5C, the GPI-GFP signal was not decreased after the analysed time period confirming intact cell adhesion. Taken together, we conclude that TIRF microscopy in combination with extensive data analysis is suitable for characterizing stimulators as well as inhibitors of GLUT4 translocation in live cells.

Identification of insulin mimetic substances

In a first attempt, we used our experimental system to characterize the effects of known insulin mimetic drugs. For these investigations, we quantified the increase in GFP fluorescence at various time intervals after adding each particular substance. Importantly, those experiments were performed in CHO-K1 cells expressing high levels of the hInsR (CHO-K1 GLUT4-myc-GFP hInsR), as well as a CHO-K1 clone exclusively expressing the endogenous insulin receptor (CHO-K1 GLUT4-myc-GFP). This approach should clarify the involvement of the insulin receptor in the efficacy of the GLUT4 translocation-modifying substances being studied.

We tested several phytochemical substances that have been shown to either influence glucose uptake or the GLUT4 translocation process (Figure 6A). We analysed the efficacy of TA (Lorrain *et al.*, 2013), a reported stimulator of GLUT4

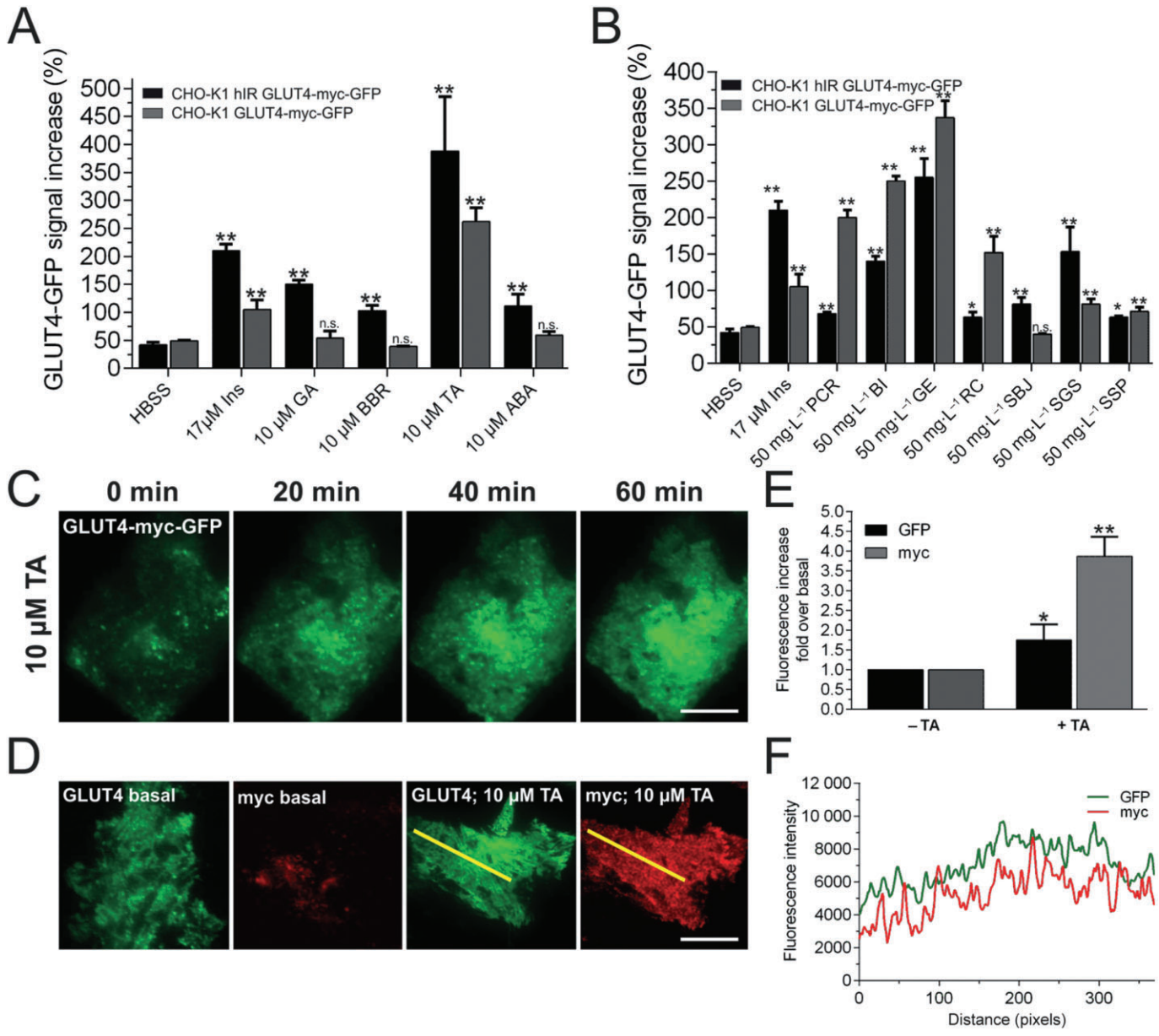

Figure 6

Characterization of insulin mimetic substances in CHO-K1 hInsR/GLUT4-myc-GFP and CHO-K1 GLUT4-myc-GFP cells. Cells were grown in 96-well plates (50 000 cells·per well) overnight, starved for 3–4 h in HBSS buffer and incubated with the indicated substance for 1 h. (A) Quantification of the increase in the GLUT4-GFP signal in the evanescent field induced by various substances with known GLUT4 translocation modulating properties. (B) Quantification of the increase in the GLUT4-GFP signal in the evanescent field induced by novel insulin mimetic substances. Error bars are based on the SEM, $n > 100$ cells. *$P < 0.05$ and **$P < 0.01$, significant increase with respect to HBSS treated cells respectively (A and B). (C) TIRF images (488 nm excitation) of a representative CHO-K1 hInsR/GLUT4-myc-GFP cell incubated with 10 µM TA at the indicated time points. (D) Representative TIRF images of CHO-K1 hInsR/GLUT4-myc-GFP cells in the absence or presence of 10 µM TA (10 min incubation time). Cells were grown in 96-well plates (50 000 cells·per well) overnight and starved for 3–4 h in HBSS. Untreated and TA stimulated cells were fixed with 4% paraformaldehyde and labelled using an Alexa647-anti-myc antibody. Excitation at 488 nm (GFP) and 640 nm (Alexa647) respectively. Scale bar = 10 µm (C and D). (E) Quantification of the fluorescence increase of the myc signal after TA application (10 µM, 10 min). (F) Fluorescence intensity profiles for the indicated line scans of a representative cell. Error bar is based on the SEM, $n > 100$ cells. *$P < 0.01$, significant increase with respect to untreated cells.

translocation in adipocytes (Liu *et al.*, 2005). An increase in GLUT4 fluorescence of about 350% occurred when 10 µM TA were applied. Figure 6C shows a representative cell that was incubated with 10 µM TA for 20, 40 and 60 min respectively. To verify that the increase in the GFP signal is mainly caused by full insertion of GLUT4 in the plasma membrane, we fixed TA-treated cells and immunostained them with a fluorescent antibody targeting the myc tag. As shown in Figure 6D, com-

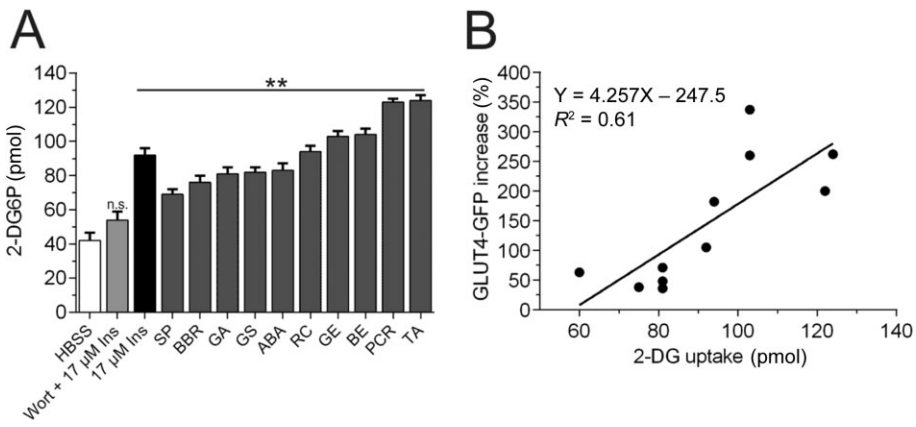

Figure 7

2-DG glucose uptake assay. (A) CHO-K1 GLUT4-myc-GFP cells were grown in 96-well plates (50 000 cells·per well) overnight and starved for 3–4 h in HBSS buffer followed by glucose deprivation with Krebs-Ringer buffer for 1 h. Cells were then stimulated with the indicated substances for 1 h followed by addition of 2-DG (20 min). Cell extracts were prepared and 2-DG uptake was measured after a colorimetric reaction using a plate reader device. Samples were measured in duplicate. Error bars are based on the SEM. $^{**}P < 0.05$, significant increase with respect to HBSS control. (B) Linear correlation regression analysis between 2-DG uptake and GLUT4-GFP increase in TIRF microscopy images.

pared with starved cells, we observed strong labelling in both colour channels when cells were incubated with 10 µM TA. In analogy to insulin treatment, we determined the extent of co-localization of GFP and the myc tag fluorescence at a single-cell level. A significant amount of co-localization was observed by line scan analysis (Figure 6F; Pearson's coefficient GFP-myc = 0.32). The increase in the myc-signal (approximately fourfold, Figure 6E) was found to be in a similar range as that observed after the application of 100 nM insulin (Figure 3B). In summary, we were able to confirm that TA indeed leads to a significantly enhanced GLUT4 insertion into the plasma membrane. Next, we incubated starved cells with the natural plant product BBR (Kuo *et al.*, 2004), which has been shown to increase AMP-activated PK activity as well as GLUT4 translocation in myotubes (Lee *et al.*, 2006). We confirmed this effect as addition of 10 µM BBR increased the GLUT4 fluorescence by ~100%. As another example, we investigated potential effects of the phenolic acid GA, which is a plant polyphenol found in gallnuts, tea leaves, oak bark and other plants. GA has been reported to induce GLUT4 translocation in adipocytes (Prasad *et al.*, 2010). In our experiments, application of 10 µM GA led to a strong increase in the GLUT4 fluorescence of ~150%. Finally, we investigated the plant hormone ABA (Milborrow, 2001), which has been reported to stimulate glucose consumption in myoblasts and adipocytes by increasing the GLUT4 levels in the plasma membrane (Bruzzone *et al.*, 2012). We found an increase of about 100% in the GLUT4 fluorescence when 10 µM ABA were added for 60 min, confirming its reported stimulating effect on GLUT4 translocation. Taken together, our approach confirmed the GLUT4 translocation stimulating properties of different plant phytochemicals.

As shown in Figure 6A, the response to insulin and the other GLUT4 translocation-inducing substances tested was found to be dependent on the expression level of the insulin receptor: The GLUT4 signal increase is remarkably lower or not detectable in CHO-K1 cells lacking high levels of the hInsR. Thus, the stimulant effects of GA, BBR, TA and ABA probably depend on the presence of this receptor.

Based on our results, we intended to identify novel phytochemicals with GLUT4 translocation stimulating properties. Therefore, we prepared different plant extracts including RC, SP, PCR, BI, GS and GE, which are especially rich in anthocyanins (Zafra-Stone *et al.*, 2007). Selected anthocyanins have been shown to ameliorate hyperglycaemia and exert insulin-like effects (Sasaki *et al.*, 2007; Scazzocchio *et al.*, 2011). As shown in Figure 6B, all these extracts markedly increased the GLUT4 signal, ranging from 75 to 250%. Interestingly, PCR, BI, GE, RC and SP extracts were found to stimulate GLUT4 translocation to a larger extent in CHO-K1 cells lacking overexpression of the hInsR, indicating an induction mechanism independent of the insulin receptor. In contrast, the stimulating effect of GS extract and SB juice was found to depend on the expression of hInsR. SB juice is especially rich in GA, whose GLUT4 translocation-promoting effect was also shown to depend on the presence of hInsR. As shown in Supporting Information Fig. S3, the concentration of the insulin receptor in the plasma membrane in CHO-K1 GLUT4-myc-GFP hInsR cells was found to be about 100% higher than in CHO-K1 GLUT4-myc-GFP cells lacking additional expression of the InsR (Supporting Information Fig. S3A and B). However, the GLUT4-myc-GFP fluorescence did not vary significantly in both CHO-K1 cell lines (Supporting Information Fig. S3C). In conclusion, using different cell models with varying insulin receptor levels provides the first insight into the underlying mechanism of this increase in GLUT4 translocatio.

Finally, we confirmed that the phytochemicals investigated do not only increase the GLUT4 fluorescence in the evanescent field, but also elevate the intracellular glucose concentration. We quantified this parameter using the 2-DG assay and found significantly elevated levels of glucose (Figure 7A). The general dependence of intracellular glucose levels on the fluorescent increase of the GLUT4 signal in TIRF

configuration can be seen by linear regression and correlation analysis. The coefficient of determination (R^2) is given in Figure 7B. The *R* value (correlation coefficient) was positive at the $P < 0.0047$ significance level, indicating that an increased GLUT4-GFP signal correlates with an elevated glucose uptake.

Discussion

Medically, the identification and characterization of new drugs that mimic the effects of insulin are much needed to prevent and treat type 2 diabetes; this applies to chemical libraries as well as the huge number of phytochemicals available. In comparison with other approaches including wet-lab techniques, fluorescence microscopy has been shown to be a valuable tool for characterizing insulin mimetic drugs, either by the application of fluorescent glucose analogues (Jung *et al.*, 2011) or more importantly by the use of fluorescent GLUT4 fusion proteins (Vijayakumar and Bhat, 2012). However, the measurement and quantification procedures that, for example, involve the use of a confocal microscopy have severely limited throughput rates.

In this study, we describe the quantification of GLUT4 translocation using TIRF microscopy. This technique offers several advantages over previously applied methods: firstly, by using an experimental set-up including an automated focus-hold system and a high-precision motorized scanning table, hundreds of cells can be analysed within a few minutes. Secondly, the increase in the fluorescence signal in the evanescent field upon insulin stimulation can be easily quantified. Finally, compared with confocal microscopy, the area of the fluorescent signal that can be quantified within a single cell is much larger. Using TIRF microscopy, we were able to accurately characterize the effects of known translocation inhibitors including wortmannin and LY294,002. In addition, we used the assay to characterize several already published as well as a number of so far not investigated natural substances with respect to their insulin mimetic properties. For our measurements, we used an insulin-sensitive cell line (CHO-K1) stably co-expressing the hInsR and a GLUT4-myc-GFP fusion protein (Vijayakumar *et al.*, 2010). To investigate live cells and to keep the method as fast and simple as possible, we mainly focused on the fluorescence of the GFP signal: we found an increase of 3–4-fold within 20–60 min. This is in line with a reported increase of the GFP signal in the evanescent field measured in adipocytes (Bai *et al.*, 2007). TIRF microscopy allows for the assessment of the GLUT4 trafficking process itself and permits the quantitative analysis of GLUT4 molecules inserted into or in close vicinity to the plasma membrane. In principal, it is unclear if the increase in fluorescence in the evanescent field in response to insulin or insulin mimetic substances is really due to an increase in GLUT4 molecules in the plasma membrane, or an elevation of docked/recruited vesicles in the TIRF zone.

To overcome this limitation, we confirmed our results by the use of three different approaches. Initially, we used the myc tag in the first extracellular loop of GLUT4 and targeted it with a fluorescent antibody. Naturally, only GLUT4 molecules inserted into the membrane can be detected in this colour channel. Utilizing dual-colour TIRF microscopy we could clearly show that an increase in the fluorescence of the GFP signal correlates well with an elevated intensity of the myc staining. This indicates that a significant amount of the GLUT4 proteins, which are released from GSCs, in fact are inserted into the plasma membrane. This holds true for stimulation of GLUT4 translocation by insulin as well as insulin mimetics: both insulin and TA resulted in increased fluorescence in the GFP and myc signal. Importantly, evidence for the improved accessibility of the myc tag after insulin stimulation was confirmed by fluorescence-guided AFM studies. Single molecular recognition force spectroscopy measurements were performed to address this question. The results from these experiments clearly demonstrated that the myc tag in the first extracellular loop is easily accessible for the antibody used only after insulin stimulation. This finding further confirms that the myc staining detected using a fluorescent antibody is correct. As an additional control, we investigated whether the increase of the GFP signal in the evanescent field also correlates with elevated glucose uptake rates. Using a 2-DG uptake assay, we confirmed that insulin stimulation results in a 2.5-fold increase in intracellular glucose levels. This effect was almost completely inhibited by wortmannin pretreatment. Different phytochemicals that were found to increase the GLUT4-GFP signal also resulted in elevated intracellular glucose concentrations. Linear regression and correlation analysis indicated that an increased GLUT4-GFP signal correlates well with an elevated glucose uptake into the used cells. Taken together, our results clearly show that quantification of the GFP signal is a valuable parameter for identifying and characterizing potential GLUT4 translocation inhibitors/stimuators. Positive hits from putative first/second round screenings have to be further evaluated by functional analyses, for example, *in vitro* glucose uptake studies similar to the 2-DG assay used here, or *in vivo* investigations on mice body weight. Both the myc staining experiments as well as the glucose uptake assay are of major importance for the significance of the GFP signal and thus for the whole study. In principle, an increased GLUT4 translocation rate induced by the identified insulin mimetics might not include the last fusion step of the GLUT4 vesicles into the plasma membrane due to the lack of insulin, which has been shown to regulate this fusion process (Lizunov *et al.*, 2009). However, our experiments clearly showed that the insulin mimetics increase the GLUT4 translocation rates as well as the number of GLUT4 proteins inserted into the plasma membrane.

We used our TIRF microscopy approach to characterize known GLUT4 translocation-modifying substances. Results confirmed (i) the GLUT4 translocation inhibitory potential of wortmannin, and LY294,002, and (ii) the promoting effects of the phytochemicals ABA, TA, BBR and GA. The latter appears of special interest due to its high bioavailability: GA is a water-soluble, well-absorbed food ingredient (Scalbert *et al.*, 2002) found in large quantities in different plants including white tea (Unachukwu *et al.*, 2010), blackberry, raspberry, wine (Mudnic *et al.*, 2012), seabuckthorn (Kumar *et al.*, 2013) and cloves (Pathak *et al.*, 2004). Furthermore, different polyphenols, for example, epigallocatechin, epicatechin gallate or gallocatechin gallate can be degraded in the colon to GA as a main product. Thus, GA is a phytochemical that is highly enriched in the human body when appropriate sources are available (Shahrzad *et al.*, 2001). In this regard, the effect of

10 μM GA (i.e. ~150% increase in GLUT4 fluorescence) seems promising. TA, a specific type of the plant polyphenol tannin that was found to be the most potent GLUT4 translocation inducer (in TIRF microscopy as well as glucose uptake studies), is also highly soluble in water and might thus serve as a promising substance to reduce blood glucose levels.

Importantly, we implemented our assay to detect and characterize novel phytochemicals with insulin mimetic properties. We prepared extracts from RC, SP, PCR, BI, GS and GE that are especially rich in anthocyanins. These phytochemicals are highly water-soluble but also thought to be subject to physiochemical degradation (Woodward *et al.*, 2009). Thus, their bioavailability *in vivo* might be lower than that of GA. However, in addition to the suggested anti-inflammatory, neuroprotective and analgesic properties (Korte *et al.*, 2009) and the amelioration of hyperglycaemia (Sasaki *et al.*, 2007), we detected a significant induction of GLUT4 translocation in our experimental conditions. 2-DG-based uptake studies confirmed the elevated intracellular glucose levels induced by these substances. In view of the availability of an enormous number of natural products, especially polyphenolic substances from fruits and tea (Kadan *et al.*, 2013), it is important to have efficient methods like the one presented here for the screening of GLUT4 translocation-modifying ingredients.

An important point that we addressed is the significance of the insulin receptor for the effects of the phytochemicals studied on GLUT4 translocation. To do this, we used two different cell lines characterized by different expression rates of the insulin receptor. While the effects of GA, TA, BBR and ABA were clearly dependent on high expression levels of the insulin receptor, several of the other plant extracts were found to stimulate GLUT4 translocation to a greater extent in CHO-K1 cells lacking overexpression of the receptor. We are convinced that this finding is an important first hint for the underlying mechanism of the stimulant effect on GLUT4 translocation. In this regard GPCRs may be candidate proteins that activate GLUT4 translocation: certain GPCRs have already been shown to cause GLUT4 forward trafficking (Liu *et al.*, 2012). Some GPCRs including GPR35, which is endogenously expressed in CHO-K1 cells and white adipose tissue (Southern *et al.*, 2013), have been found to be activated by natural substances that were also tested in this study (Deng and Fang, 2012). Further in-depth studies are needed to unravel the role of such GPCRs in the activation of GLUT4 translocation induced by phytochemicals. However, although of great interest, the relevance of the insulin and other receptors for GLUT4 translocation-activating substances will be a major task for upcoming research activities. The TIRF microscopy-based approach presented here appears to be an excellent tool to lay the foundation for these investigations.

In summary, we present here a holistic approach for the study of GLUT4 translocation-modifying substances, and have used our assay to find novel inducers of this translocation. The quality of the procedure is affected by the combination of individual components: (i) application of an insulin-sensitive, GLUT4-overexpressing cell line that grows fast without the need for differentiation, (ii) analysis of live or fixed cells, (iii) utilization of a TIRF microscopy set-up with an automated focus-hold system, a high-precision motorized scanning table and a mounting system designed for the microplate format and (iv) quantification of results by use of customized software. The limitation concerning the availability of user-friendly TIRF microscopes, which is sometimes raised, actually is of no consequence: modern TIRF set-ups are fully automated and possibly as controllable as any other fluorescence microscopy technology. Furthermore, TIRF in microplates has already been successfully used for drug screening of fluorescently labelled GPCRs (Chen *et al.*, 2013). Thus, TIRF microscopy-guided screening for insulin mimetic drugs appears to be a viable option for the development of new drugs, where acceptable throughput rates are an absolute necessity.

Acknowledgements

This work was carried out in the frame of Regio13 and financially supported by the European Regional Development Fund (EFRE) and the state of Upper Austria. Verena Stadlbauer is a recipient of a 'FEMtech Praktikum' funded by the Austrian Research Promotion Agency (FFG). We thank Manoj Kumar Bhat (National Centre for Cell Science, NCCS Complex, Pune University, India) for providing the CHO-K1 hInsR GLUT4-myc-GFP cell line. Phytochemical extracts were kindly provided by Thomas Eidenberger (Belan GmbH, Wels, Austria). We thank Mario Brameshuber (Technical University Vienna, Austria) for critically reading the manuscript.

Author contributions

P. L., V. S., O. H., K. S., P. H. and J. We. conceived and designed the experiments. P. L., V. S., L. A. C., R. H. and J. We. performed the experiments. P. L., V. S., L. A. C., D. B., S. M. W., J. Wr. and J. We. analysed the data. P. L. and J. We. wrote the manuscript.

Conflict of interest

The authors declare no conflict of interest.

References

Alexander SPH, Benson HE, Faccenda E, Pawson AJ, Sharman JL, Spedding M *et al.* (2013a). The Concise Guide to PHARMACOLOGY 2013/14: G protein-coupled receptors. Br J Pharmacol 170: 1459–1581.

Alexander SPH, Benson HE, Faccenda E, Pawson AJ, Sharman JL, Spedding M *et al.* (2013b). The Concise Guide to PHARMACOLOGY 2013/14: catalytic receptors. Br J Pharmacol 170: 1676–1705.

Alexander SPH, Benson HE, Faccenda E, Pawson AJ, Sharman JL, Spedding M *et al.* (2013c). The Concise Guide to PHARMACOLOGY 2013/14: transporters. Br J Pharmacol 170: 1706–1796.

Bai L, Wang Y, Fan J, Chen Y, Ji W, Qu A *et al.* (2007). Dissecting multiple steps of GLUT4 trafficking and identifying the sites of insulin action. Cell Metab 5: 47–57.

Baus D, Heermeier K, De Hoop M, Metz-Weidmann C, Gassenhuber J, Dittrich W *et al*. (2008). Identification of a novel AS160 splice variant that regulates GLUT4 translocation and glucose-uptake in rat muscle cells. Cell Signal 20: 2237–2246.

Bruzzone S, Ameri P, Briatore L, Mannino E, Basile G, Andraghetti G *et al*. (2012). The plant hormone abscisic acid increases in human plasma after hyperglycemia and stimulates glucose consumption by adipocytes and myoblasts. FASEB J 26: 1251–1260.

Bryant NJ, Govers R, James DE (2002). Regulated transport of the glucose transporter GLUT4. Nat Rev Mol Cell Biol 3: 267–277.

Carvalho E, Schellhorn SE, Zabolotny JM, Martin S, Tozzo E, Peroni OD *et al*. (2004). GLUT4 overexpression or deficiency in adipocytes of transgenic mice alters the composition of GLUT4 vesicles and the subcellular localization of GLUT4 and insulin-responsive aminopeptidase. J Biol Chem 279: 21598–21605.

Chen M, Zaytseva NV, Wu Q, Li M, Fang Y (2013). Microplate-compatible total internal reflection fluorescence microscopy for receptor pharmacology. Appl Phys Lett 102: 193702.

Chen Y, Wang Y, Zhang J, Deng Y, Jiang L, Song E *et al*. (2012). Rab10 and myosin-Va mediate insulin-stimulated GLUT4 storage vesicle translocation in adipocytes. J Cell Biol 198: 545–560.

Chtcheglova LA, Atalar F, Ozbek U, Wildling L, Ebner A, Hinterdorfer P (2008). Localization of the ergtoxin-1 receptors on the voltage sensing domain of hERG K + channel by AFM recognition imaging. Pflugers Arch 456: 247–254.

Chtcheglova LA, Wildling L, Waschke J, Drenckhahn D, Hinterdorfer P (2010). AFM functional imaging on vascular endothelial cells. J Mol Recognit 23: 589–596.

Clarke JF, Young PW, Yonezawa K, Kasuga M, Holman GD (1994). Inhibition of the translocation of GLUT1 and GLUT4 in 3T3-L1 cells by the phosphatidylinositol 3-kinase inhibitor, wortmannin. Biochem J 300 (Pt 3): 631–635.

Creager MA, Luscher TF, Cosentino F, Beckman JA (2003). Diabetes and vascular disease: pathophysiology, clinical consequences, and medical therapy: part I. Circulation 108: 1527–1532.

Deng H, Fang Y (2012). Anti-inflammatory gallic acid and wedelolactone are G protein-coupled receptor-35 agonists. Pharmacology 89: 211–219.

Giebel K, Bechinger C, Herminghaus S, Riedel M, Leiderer P, Weiland U *et al*. (1999). Imaging of cell/substrate contacts of living cells with surface plasmon resonance microscopy. Biophys J 76 (1 Pt 1): 509–516.

Jiang ZY, Chawla A, Bose A, Way M, Czech MP (2002). A phosphatidylinositol 3-kinase-independent insulin signaling pathway to N-WASP/Arp2/3/F-actin required for GLUT4 glucose transporter recycling. J Biol Chem 277: 509–515.

Jung DW, Ha HH, Zheng X, Chang YT, Williams DR (2011). Novel use of fluorescent glucose analogues to identify a new class of triazine-based insulin mimetics possessing useful secondary effects. Mol Biosyst 7: 346–358.

Kadan S, Saad B, Sasson Y, Zaid H (2013). In vitro evaluations of cytotoxicity of eight antidiabetic medicinal plants and their effect on GLUT4 translocation. Evid Based Complement Alternat Med 2013: 549345.

Kahn SE, Hull RL, Utzschneider KM (2006). Mechanisms linking obesity to insulin resistance and type 2 diabetes. Nature 444: 840–846.

Klip A (2009). The many ways to regulate glucose transporter 4. Appl Physiol Nutr Metab 34: 481–487.

Korte G, Dreiseitel A, Schreier P, Oehme A, Locher S, Hajak G *et al*. (2009). An examination of anthocyanins' and anthocyanidins' affinity for cannabinoid receptors. J Med Food 12: 1407–1410.

Kristiansen S, Richter EA (2002). GLUT4-containing vesicles are released from membranes by phospholipase D cleavage of a GPI anchor. Am J Physiol Endocrinol Metab 283: E374–E382.

Kumar MS, Praveenkumar R, Ilavarasi A, Rajeshwari K, Thajuddin N (2013). Biochemical changes of fresh water cyanobacteria Dolichospermum flos-aquae NTMS07 to chromium-induced stress with special reference to antioxidant enzymes and cellular fatty acids. Bull Environ Contam Toxicol 90: 730–735.

Kuo CL, Chi CW, Liu TY (2004). The anti-inflammatory potential of berberine in vitro and in vivo. Cancer Lett 203: 127–137.

Lampson MA, Racz A, Cushman SW, McGraw TE (2000). Demonstration of insulin-responsive trafficking of GLUT4 and vpTR in fibroblasts. J Cell Sci 113 (Pt 22): 4065–4076.

Lampson MA, Schmoranzer J, Zeigerer A, Simon SM, McGraw TE (2001). Insulin-regulated release from the endosomal recycling compartment is regulated by budding of specialized vesicles. Mol Biol Cell 12: 3489–3501.

Lanzerstorfer P, Borgmann D, Steininger A, Schaller S, Brameshuber M, Sunzenauer S *et al*. (eds) (2013). Analysis of protein-protein interactions in live cells – the µ-patterning approach. iConcept Press.

Lanzerstorfer P, Borgmann D, Schutz G, Winkler SM, Hoglinger O, Weghuber J (2014). Quantification and kinetic analysis of Grb2-EGFR Interaction on micro-patterned surfaces for the characterization of EGFR-modulating substances. PLoS ONE 9: e92151.

Lee YS, Kim WS, Kim KH, Yoon MJ, Cho HJ, Shen Y *et al*. (2006). Berberine, a natural plant product, activates AMP-activated protein kinase with beneficial metabolic effects in diabetic and insulin-resistant states. Diabetes 55: 2256–2264.

Liu D, Wang L, Meng Q, Kuang H, Liu X (2012). G-protein coupled receptor 120 is involved in glucose metabolism in fat cells. Cell Mol Biol (Noisy-Le-Grand) Suppl. 58: OL1757–OL1762.

Liu F, Dallas-Yang Q, Castriota G, Fischer P, Santini F, Ferrer M *et al*. (2009). Development of a novel GLUT4 translocation assay for identifying potential novel therapeutic targets for insulin sensitization. Biochem J 418: 413–420.

Liu X, Kim JK, Li Y, Li J, Liu F, Chen X (2005). Tannic acid stimulates glucose transport and inhibits adipocyte differentiation in 3T3-L1 cells. J Nutr 135: 165–171.

Lizunov VA, Lisinski I, Stenkula K, Zimmerberg J, Cushman SW (2009). Insulin regulates fusion of GLUT4 vesicles independent of Exo70-mediated tethering. J Biol Chem 284: 7914–7919.

Lorrain B, Ky I, Pechamat L, Teissedre PL (2013). Evolution of analysis of polyphenols from grapes, wines, and extracts. Molecules 18: 1076–1100.

Maira SM, Stauffer F, Schnell C, Garcia-Echeverria C (2009). PI3K inhibitors for cancer treatment: where do we stand? Biochem Soc Trans 37 (Pt 1): 265–272.

Milborrow BV (2001). The pathway of biosynthesis of abscisic acid in vascular plants: a review of the present state of knowledge of ABA biosynthesis. J Exp Bot 52: 1145–1164.

Mudnic I, Budimir D, Modun D, Gunjaca G, Generalic I, Skroza D *et al*. (2012). Antioxidant and vasodilatory effects of blackberry and grape wines. J Med Food 15: 315–321.

Pathak SB, Niranja K, Padh H, Rajani M (2004). TLC densitometric method for the quantification of eugenol and gallic acid in clove. Chromatographia 60: 241–244.

Pawson AJ, Sharman JL, Benson HE, Faccenda E, Alexander SP, Buneman OP *et al.*; NC-IUPHAR (2014). The IUPHAR/BPS Guide to PHARMACOLOGY: an expert-driven knowledgebase of drug targets and their ligands. Nucl Acids Res 42 (Database Issue): D1098–D1106.

Pessin JE, Saltiel AR (2000). Signaling pathways in insulin action: molecular targets of insulin resistance. J Clin Invest 106: 165–169.

Prasad CN, Anjana T, Banerji A, Gopalakrishnapillai A (2010). Gallic acid induces GLUT4 translocation and glucose uptake activity in 3T3-L1 cells. FEBS Lett 584: 531–536.

Puntheeranurak T, Wildling L, Gruber HJ, Kinne RK, Hinterdorfer P (2006). Ligands on the string: single-molecule AFM studies on the interaction of antibodies and substrates with the Na+-glucose co-transporter SGLT1 in living cells. J Cell Sci 119 (Pt 14): 2960–2967.

Sasaki R, Nishimura N, Hoshino H, Isa Y, Kadowaki M, Ichi T *et al.* (2007). Cyanidin 3-glucoside ameliorates hyperglycemia and insulin sensitivity due to downregulation of retinol binding protein 4 expression in diabetic mice. Biochem Pharmacol 74: 1619–1627.

Scalbert A, Morand C, Manach C, Remesy C (2002). Absorption and metabolism of polyphenols in the gut and impact on health. Biomed Pharmacother 56: 276–282.

Scazzocchio B, Vari R, Filesi C, D'Archivio M, Santangelo C, Giovannini C *et al.* (2011). Cyanidin-3-O-beta-glucoside and protocatechuic acid exert insulin-like effects by upregulating PPARgamma activity in human omental adipocytes. Diabetes 60: 2234–2244.

Shahrzad S, Aoyagi K, Winter A, Koyama A, Bitsch I (2001). Pharmacokinetics of gallic acid and its relative bioavailability from tea in healthy humans. J Nutr 131: 1207–1210.

Smyth S, Heron A (2006). Diabetes and obesity: the twin epidemics. Nat Med 12: 75–80.

Southern C, Cook JM, Neetoo-Isseljee Z, Taylor DL, Kettleborough CA, Merritt A *et al.* (2013). Screening beta-arrestin recruitment for the identification of natural ligands for orphan G-protein-coupled receptors. J Biomol Screen 18: 599–609.

Stockli J, Fazakerley DJ, James DE (2011). GLUT4 exocytosis. J Cell Sci 124 (Pt 24): 4147–4159.

Unachukwu UJ, Ahmed S, Kavalier A, Lyles JT, Kennelly EJ (2010). White and green teas (Camellia sinensis var. sinensis): variation in phenolic, methylxanthine, and antioxidant profiles. J Food Sci 75: C541–C548.

Vijayakumar MV, Bhat MK (2012). Real time qualitative and quantitative GLUT4 translocation assay. Methods Enzymol 505: 257–271.

Vijayakumar MV, Ajay AK, Bhat MK (2010). Demonstration of a visual cell-based assay for screening glucose transporter 4 translocation modulators in real time. J Biosci 35: 525–531.

Weghuber J, Aichinger MC, Brameshuber M, Wieser S, Ruprecht V, Plochberger B *et al.* (2011). Cationic amphipathic peptides accumulate sialylated proteins and lipids in the plasma membrane of eukaryotic host cells. Biochim Biophys Acta 1808: 2581–2590.

Wildling L, Unterauer B, Zhu R, Rupprecht A, Haselgrubler T, Rankl C *et al.* (2011). Linking of sensor molecules with amino groups to amino-functionalized AFM tips. Bioconjug Chem 22: 1239–1248.

Wildling L, Rankl C, Haselgrubler T, Gruber HJ, Holy M, Newman AH *et al.* (2012). Probing binding pocket of serotonin transporter by single molecular force spectroscopy on living cells. J Biol Chem 287: 105–113.

Woodward G, Kroon P, Cassidy A, Kay C (2009). Anthocyanin stability and recovery: implications for the analysis of clinical and experimental samples. J Agric Food Chem 57: 5271–5278.

Xiong W, Jordens I, Gonzalez E, McGraw TE (2010). GLUT4 is sorted to vesicles whose accumulation beneath and insertion into the plasma membrane are differentially regulated by insulin and selectively affected by insulin resistance. Mol Biol Cell 21: 1375–1386.

Zafra-Stone S, Yasmin T, Bagchi M, Chatterjee A, Vinson JA, Bagchi D (2007). Berry anthocyanins as novel antioxidants in human health and disease prevention. Mol Nutr Food Res 51: 675–683.

Supporting information

Additional Supporting Information may be found in the online version of this article at the publisher's web-site:

http://dx.doi.org/10.1111/bph.12845

Figure S1 Influence of varying starving and buffer conditions on GLUT4-GFP signal increase. The average GFP fluorescence in the evanescent field was measured in CHO-K1 GLUT4-myc-GFP hInsR cells grown overnight in medium including serum (50 000 cells·per well), the same cells starved in medium without serum or HBSS buffer respectively (first three bars). Addition of 100 nM insulin dissolved in HBSS or KRPH buffer for 10 min resulted in a similar fluorescence as determined for cells grown in full medium (bars four and five).

Figure S2 Specificity of GLUT4-GFP signal increase after insulin stimulation. The indicated cell line was grown in 96-well plates (50 000 cells·per well) overnight and then starved for 3–4 h in HBSS buffer followed by insulin treatment. (A) Representative TIRF microscopy images of starved and insulin-treated (100 nM, 60 min) CHO-K1 cells expressing CD147-YFP, GPI-GFP and EGFR-GFP respectively. Scale bar = 10 μm. (B) Time course of the fluorescence signal of the aforementioned CHO-K1 cells. Fluorescence was normalized to value prior to insulin application. Error bars are based on the SEM, $n > 300$ cells.

Figure S3 Comparison of insulin receptor and GLUT4-myc-GFP expression rates in CHO-K1 GLUT4-myc-GFP and CHO-K1 GLUT4-myc-GFP hInsR cells. The indicated cells were grown in 96-well plates (50 000 cells·per well) overnight, followed by incubation with an anti-InsR Alexa647 antibody prior to TIRF microscopy. (A) Representative TIRF microscopy images of both cell lines labelled with an anti-InsR Alexa647 antibody. Scale bar = 7 μm. (B) Quantification of the respective anti-InsR Alexa647 signals. $^{**}P < 0.01$, significant difference with respect to CHO-K1 GLUT4-myc-GFP cells. (C) Quantification of the GLUT4-myc-GFP fluorescence intensity in both cell lines. Error bars are based on the SEM, $n > 500$ cells each.